Is the Human Operator in a Teleoperation System Passive?

Matthew Dyck* IEEE Student Member
Ali Jazayeri† IEEE Student Member
Mahdi Tavakoli‡ IEEE Member

Department of Electrical and Computer Engineering
University of Alberta

ABSTRACT

Conventional approaches for stability analysis of bilateral teleoperation systems assume that the human operator does not inject energy into the system and behaves in a passive manner. Does this assumption hold for various tasks the human operator may execute in a teleoperation context? To answer this question, in this paper we measure the endpoint impedance (inertia, viscosity, and stiffness) of the human arm during two tasks: (1) *relaxed grasping* of a haptic device while the device imposes position perturbations, and (2) *rigid grasping* of a haptic device (posture maintenance) while the device imposes force perturbations. The human arm impedance is identified as a 2×2 transfer function matrix and assessed for passivity over the frequency range characteristic of human motion. Our results agree with previous findings that the relaxed human arm behaves as a passive system. However, whether the rigid arm behaves as an active or passive system is found to depend on the magnitude of the force perturbations. We discuss why the passivity of the human operator is task dependent.

Index Terms: H.1.2 [Information Systems]: User/Machine Systems—Human Factors; I.6.4 [Simulation and Modeling]: Model Validation and Analysis

1 INTRODUCTION

A teleoperation system consists of a human operator, a remote environment, and a teleoperator. In this definition, the teleoperator comprises a master and a slave robot, their controllers, and a communication channel.

The stability of a bilateral haptic teleoperation system may be investigated by applying the passivity (Raisbeck's or scattering-based) criterion or the absolute stability (Llewellyn's) criterion to the teleoperator [3, 8]. In both frameworks, *passivity of the teleoperator's terminations, i.e., the human operator and the environment, is assumed*. This is simply a convenient yet necessary assumption for stability analysis of a teleoperation system independent of the typically uncertain, time-varying and/or unknown dynamics of two of its subsystems—the human operator and the environment. However, given that the human operator voluntarily manipulates the master robot and thereby has the capacity to inject energy into the teleoperation system, is the assumption of human operator passivity indeed valid for any task?

To address this question, the human arm's mechanical impedance (the dynamic relationship between force and motion) can be empirically measured and assessed for passivity. Several researchers have developed techniques to measure the endpoint impedance of the human arm in a plane by analyzing the arm's response to force or position perturbations imposed on the hand by a robot. A two-dimensional impedance measurement has been found sufficient to facilitate analysis of the relative contributions of the shoulder, elbow, and biarticular muscles to the overall limb impedance without necessitating the experimental complexity of a full three-dimensional measurement [9]. So far, three main applications have motivated research in human arm impedance modeling: characterizing arm dynamics to design human-robot interaction systems [5, 10], investigating how the central nervous system (CNS) controls movement [7, 13], and assessing the motor function of impaired individuals undergoing neurorehabilitation therapy [1, 14].

Mussa-Ivaldi et al. [13] used a planar robot to impose position step perturbations on a human subject's arm and measure the resulting restoring forces. They used this data to calculate the static stiffness of the arm in two Cartesian dimensions. Subjects were instructed to relax their arm and avoid voluntarily intervening as the robot perturbed their hand. Hogan [10] extended this work by decomposing the measured stiffness into an active and a passive component. The active component was found to be negligibly small in comparison to the passive component, demonstrating that the relaxed human arm behaves as a passive system. McIntyre et al. [12] adapted the technique of Mussa-Ivaldi et al. to measure changes in stiffness in response to external loading forces. Gomi et al. [7], Dolan et al. [5], and Tsuji et al. [15] extended the same approach to measure not only the arm's stiffness, but also its inertia and viscosity. Several researchers have since employed stochastic position [1] or force perturbations [14] to identify non-parametric models of arm impedance or admittance and to develop detailed models of the arm's neuromusculoskeletal structure [4]. This paper contributes to previous work by: (1) measuring arm impedance as the human performs both relaxed grasping and rigid grasping tasks, (2) performing a detailed passivity analysis of the identified dynamic impedance models, and (3) explicitly considering how the robot impedance, robot controller, and CNS position control dynamics influence the measured impedance of the human arm.

2 MATHEMATICAL PRELIMINARIES

For purposes of analyzing passivity, it is useful to employ a parametric impedance model such that the identified parameters have direct physical meaning. In this paper, arm impedance in a Cartesian plane is modeled as follows:

$$\mathbf{M}\frac{d^2}{dt^2}X(t)+\mathbf{B}\frac{d}{dt}X(t)+\mathbf{K}(X(t)-X_v)=-F(t), \qquad (1)$$

where $X(t)=[x(t)\,y(t)]^T$ is the hand position, $F(t)=[f_x(t)\,f_y(t)]^T$ is the force the hand exerts on the robot, and $X_v=[x_v\;y_v]^T$ is the hand equilibrium position commanded by the CNS. The matrices $\mathbf{M}$, $\mathbf{B}$, and $\mathbf{K}$, which represent the hand inertia, damping, and stiffness, respectively, contain real-valued constants for the Cartesian plane of measurement:

$$\mathbf{M}\doteq\begin{bmatrix}m_{xx} & m_{xy}\\ m_{yx} & m_{yy}\end{bmatrix},\ \mathbf{B}\doteq\begin{bmatrix}b_{xx} & b_{xy}\\ b_{yx} & b_{yy}\end{bmatrix},\ \mathbf{K}\doteq\begin{bmatrix}k_{xx} & k_{xy}\\ k_{yx} & k_{yy}\end{bmatrix}. \qquad (2)$$

This impedance model is derived from a simplified model of the human arm's neuromusculoskeletal structure, as Dolan et al. detail

*e-mail: matthew.dyck@ualberta.ca
†e-mail: ali.jazayeri@ualberta.ca
‡e-mail: mahdi.tavakoli@ualberta.ca

IEEE World Haptics Conference 2013
14-18 April, Daejeon, Korea
978-1-4799-0088-6/13/$31.00 ©2013 IEEE

in [5]. The equation can also be interpreted as second-order Taylor-series linearization of an arbitrary nonlinear impedance model. Due to the constant **M**, **B**, and **K** matrices, this model accurately describes the arm's dynamics for small, brief perturbations about an operating point.

At time t_0 immediately before the onset of a position or force perturbation imposed on the arm by the haptic device, (1) becomes:

$$\mathbf{M}\frac{d^2}{dt^2}X(t_0)+\mathbf{B}\frac{d}{dt}X(t_0)+\mathbf{K}(X(t_0)-X_v)=-F(t_0). \qquad (3)$$

Eliminating X_v from (1) and (3) yields:

$$\mathbf{M}\frac{d^2}{dt^2}\delta X(t)+\mathbf{B}\frac{d}{dt}\delta X(t)+\mathbf{K}(\delta X(t))=-\delta F(t), \qquad (4)$$

where $\delta X(t) \doteq X(t)-X(t_0)$ and $\delta F(t) \doteq F(t)-F(t_0)$. Being independent of the hand's equilibrium position X_v, the impedance matrices of the human arm are identified from (4).

For passivity analysis, we require the relation between the power conjugate variables of force and velocity. Taking the Laplace transform of (4) and defining $F(s) \doteq \mathscr{L}\{F(t)\}$ and $V(s) \doteq \mathscr{L}\{\dot{\delta X}(t)\}$, the arm impedance can be represented as the transfer function matrix

$$Z(s)=\begin{bmatrix} \dfrac{m_{xx}s^2+b_{xx}s+k_{xx}}{s} & \dfrac{m_{xy}s^2+b_{xy}s+k_{xy}}{s} \\ \dfrac{m_{yx}s^2+b_{yx}s+k_{yx}}{s} & \dfrac{m_{yy}s^2+b_{yy}s+k_{yy}}{s} \end{bmatrix}, \qquad (5)$$

with $F(s)=Z(s)V(s)$.

For a transfer function matrix to represent a passive system, it must be positive real [2] as defined below.

Definition 1. [2] An $n \times n$ rational transfer function matrix $G(s)$ is positive real if:

(i) the poles of all elements of $G(s)$ are in $Re[s] \leq 0$,
(ii) for all real positive frequencies ω for which $j\omega$ is not a pole of any element of $G(s)$, the matrix $H(j\omega) \doteq G(j\omega)+G^T(-j\omega)$ is positive semidefinite, and
(iii) any pure imaginary pole $j\omega$ of any element of $G(s)$ is a simple pole, and the residue matrix $\lim_{s\to j\omega}(s-j\omega)G(s)$ is positive semidefinite Hermitian.

3 Human Arm Impedance Identification

3.1 Experiment Setup

Impedance measurements were performed with a two degree-of-freedom (DOF) planar robot and haptic device manufactured by Quanser, Inc. (Markham, Ontario, Canada). Designed for neurorehabilitation exercises, the robot's capstan drive mechanism makes it readily back-drivable with low friction and inertia. At its endpoint, the robot can exert forces in excess of 50 N throughout the semicircular workspace, and the motors' optical encoders provide a Cartesian resolution of better than 0.002 mm in position measurement. The robot may be position controlled by a feedback-linearized position controller or force controlled in open loop by translating a commanded Cartesian force into required motor torques through the robot's Jacobian transpose matrix. A 2-DOF force sensor was constructed by mounting strain gauges on an aluminum post connecting the robot's distal link to the handle grasped by the human. The sensor has a resolution of 0.04 N, maximum measurable force of 75 N, and nearly linear input-output characteristic over its operating range. All data logging and robot control actions occurred with a 1 kHz sampling frequency.

For arm impedance identification, data was collected from a 23-year-old right-handed male with no history of motor impairment. In each trial, the subject sat in front of the robot and grasped the device's hemispherical handle with his right hand. The subject's elbow was supported against gravity by a sling attached to a 2 m rope connected to the ceiling. All data was collected at a *test location* ($x = 0$ cm, $y = 52$ cm) in a coordinate frame aligned at the subject's shoulder joint (Fig. 1). A belt restrained the subject's torso to the prevent translation of the upper body, which would have undermined the accuracy of the arm position measurements.

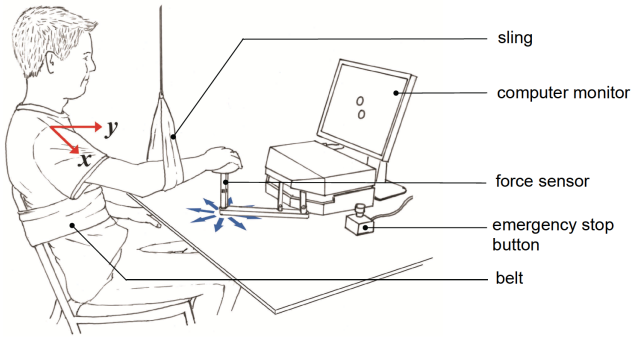

Figure 1: Experimental apparatus for human arm impedance measurements. Red arrows indicate the measurement coordinate frame. Blue arrows show the directions of applied perturbations. Measurements are performed in a horizontal plane approximately 10 cm below the shoulder joint.

3.2 Data Collection

Two types of motor control tasks were investigated in our study. The relaxed grasping task required the subject to relax his arm while the robot applied position perturbations, just as a human operator in a teleoperation system might relax his arm to enhance perception of haptic feedback from the slave and environment. In the rigid grasping task, the subject sought to minimize the displacement of his hand while the robot applied force perturbations, as might be required to haptically teleoperate a vehicle in rough terrain or haptically teleoperate a drill.

Relaxed grasping Inspired by the experiments in [5], the robot applied step-like, rapidly-rising, underdamped position perturbations to the subject's hand. The commanded steady-state amplitude of each perturbation was 5 mm, but hand displacements of up to 11 mm were observed during the transient portion of the motion. Two perturbations were applied in each of 8 directions spaced evenly at 45° intervals around a circle, for a total of 16 perturbations per trial. The subject was instructed to relax while the robot applied the perturbations. To reduce any subconscious intervention on the part of the subject, the 16 perturbations were applied in random order. For the same reason, each perturbation's duration (1.5–2.0 s) and onset time (2.0–7.0 s after the previous perturbation) were selected randomly. Following each perturbation, the robot's position controller gently moved the subject's hand back to the test location such that each subsequent perturbation was delivered from exactly the same initial position.

The force sensor measured the sum of forces exerted by the human arm and inertial contributions from the robot's handle and the sensor structure. Therefore, the experiment was repeated *without* the subject grasping the robot (i.e., in free space) to quantify these inertial contributions such that their effects could later be removed when calculating the impedance.

Rigid grasping In the rigid grasping task, a computer monitor displayed a circle representing the robot's handle position (i.e., the subject's hand position) and a circle corresponding to the test location. Using this visual feedback, the subject was instructed to keep his hand centered at the test location while the robot exerted force

perturbations. Step-like underdamped force perturbations were applied with their duration, onset, and direction selected randomly as in the relaxed grasping experiment. The commanded steady-state amplitude of the force perturbations was either 2 N or 5 N, with the measured interaction forces during the transient phase being as large as 6 N or 13 N, respectively.

The relaxed grasping, 2 N rigid grasping, and 5 N rigid grasping experiments were each repeated five times for a total of 15 trials. Typical force and position trajectories are shown in Fig. 2.

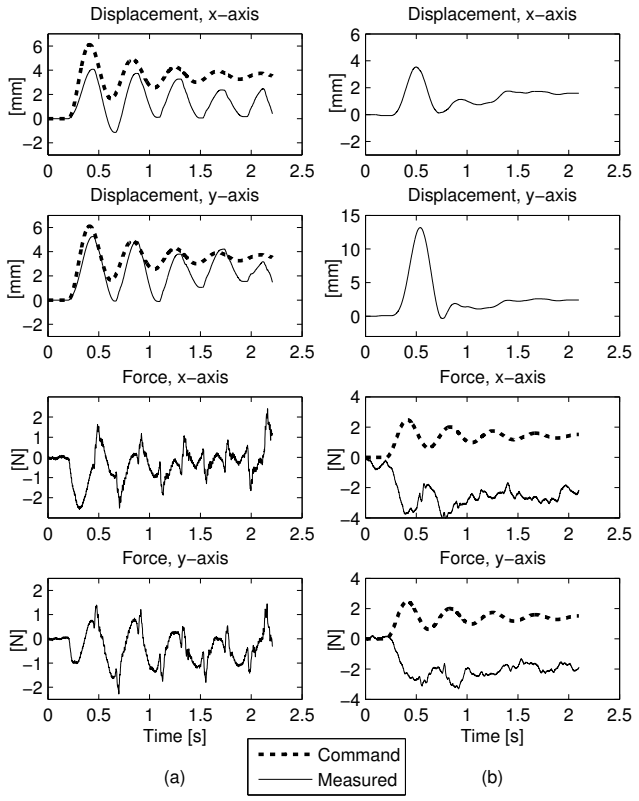

Figure 2: Typical force and position signals for (a) relaxed grasping and (b) rigid grasping with 2 N perturbations. Forces have been low-pass filtered to reduce noise. Dashed lines indicate the command signals to the robot's position or force controller. As the force sensor measures the force exerted *by the human on the robot*, the measured force in (b) is the negative of the force the *robot is commanded to exert on the human*.

3.3 Identification Technique

The data used to identify human arm impedance is collected from a closed-loop system. The force sensor measures the total force the human exerts on the robot, $F_h = F_h^* - Z_h X$, where F_h^* is the human's voluntary force contribution, Z_h the human's impedance, and X the displacement from the test location. During relaxed grasping (Fig. 3a), the robot's position controller C_r tracks a perturbation signal X_r^*, causing the robot to exert a force F_r^* and move to position X. Since the human does not consciously intervene in the process, his voluntary force contribution F_h^* is zero. Therefore, since $F_h = -Z_h X$ and both F_h and X are measured, Z_h can be identified directly from the closed-loop data according to (4).

In the rigid grasping task (Fig. 3b), the human is instructed to minimize displacements ($X_h^* = 0$) in the face of robotic force perturbations F_r^*. When these forces act on the admittance of the human arm to move the hand away from the test location to a position X, the CNS (modeled by position controller C_h in Fig. 3b)

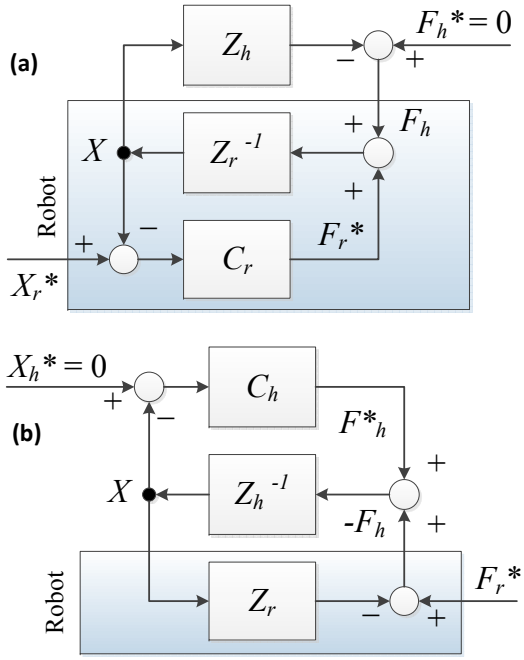

Figure 3: Dynamics of (a) a relaxed grasping task with position perturbations (robot is closed-loop position controlled) and (b) a rigid grasping task with force perturbations (robot is open-loop force controlled). Human and robot impedances are Z_h and Z_r, respectively. The force sensor measures F_h, the force exerted by the human on the robot. See text for definition of other variables.

responds by causing the human to consciously exert a force F_h^* to counteract this motion. A negative feedback loop from $-F_h$ to X thus exists, with Z_h^{-1} in the feedforward path and C_h in the negative feedback path, such that $\frac{X}{-F_h} = \frac{Z_h^{-1}}{1+Z_h^{-1}C_h}$. This expression simplifies to $F_h = -(C_h + Z_h)X$. In other words, the identification results for a rigid grasping task are influenced by both the physical properties of the arm (Z_h, which arises from the arm's intrinsic mechanics and involuntary reflex responses) and the dynamics introduced by the human's voluntary position control response (C_h). While the identified model can still be termed an "impedance" since it relates a position input to a force output, the CNS dynamics are subsumed into the identified impedance matrices.

The matrices **M**, **B**, and **K** in (4) were identified by linear regression. Prior to the least-squares identification, the force signals were noise-filtered forward and backward (MATLAB function *filtfilt*) by a 10$^{\text{th}}$ order Butterworth low-pass filter with a cutoff frequency of 20 Hz. To reduce effects of noise and gradual measurement drift when calculating $\delta X(t)$ and $\delta F(t)$ in (4), the average values of $X(t)$ and $F(t)$ for the last 100 ms immediately prior to each perturbation were subtracted from $X(t)$ and $F(t)$ recorded during the perturbation. Time-derivatives of $\delta X(t)$ were subsequently calculated through a state-variable filtering technique described in [5].

To quantify what portion of the measured force was due to the inertial contributions from the handle and the force sensor structure, the force-position data collected from the robot's motion in free space (see Section 3.2) was fit to the following equation:

$$\Lambda \frac{d^2}{dt^2} \delta X(t) = -\delta F(t), \tag{6}$$

yielding the effective inertia of the handle and the force sensor structure as $\Lambda = 199.1 \pm 0.5$ g.

The human arm's inertia, damping, and stiffness matrices were subsequently identified by applying the least-squares procedure to

$$(\mathbf{M}+\Lambda\mathbf{I})\frac{d^2}{dt^2}\delta X(t)+\mathbf{B}\frac{d}{dt}\delta X(t_0)+\mathbf{K}(\delta X(t))=-\delta F(t), \quad (7)$$

where $\mathbf{I}$ is the 2×2 identity matrix. Only the first 1.5 s of data from each perturbation was included in the identification, which was found to be more than sufficient for parameter estimates to converge to steady values.

3.4 Validation of Identification Technique

The data collection and impedance measurement techniques were validated against a mechanical spring array with known impedance. Several linear springs were connected to the handle of the robot to create a two-dimensional stiffness field comparable to that of the human arm. The robot applied a series of position perturbations as in the relaxed grasping task. The measured stiffness matrix $\mathbf{K}$ was compared to the theoretical stiffness matrix calculated from an independent measurement of the spring constants. Over multiple trials with different spring configurations, the percent discrepancy between the 2-norms of the measured and theoretical stiffness matrices was consistently less than 8%.

4 Results

4.1 Identified Human Arm Impedances

Identified impedance matrices for each trial are shown in Table 1. The elements of the stiffness and damping matrices were generally larger for rigid grasping compared to relaxed grasping, which was expected as arm stiffness and damping increase with grip strength [15]. The inertia values measured in the rigid grasping were typically smaller than those for relaxed grasping, especially when 5 N force perturbations were applied. The rigid grasping impedance measurements also show higher inter-trial variability. The complex dynamics of the CNS position control response account for this increased variability, as discussed later.

While it is conventional to measure arm impedance in the horizontal plane at the elevation of the shoulder (e.g. [5, 13]), the equipment used in this study necessitated performing measurements approximately 10 cm below the shoulder. However, this height differential has been shown to have only a minor impact on the measured impedance [6]. Indeed, for the relaxed task, our results are comparable to those obtained by other researchers under similar conditions [6, 15] and are fairly consistent between trials.

4.2 Passivity Analysis

The stiffness matrix in (2) can be separated into a symmetric and a skew-symmetric component as

$$\mathbf{K_s}=\begin{bmatrix} k_{xx} & \frac{k_{xy}+k_{yx}}{2} \\ \frac{k_{yx}+k_{xy}}{2} & k_{yy}\end{bmatrix}, \quad \mathbf{K_a}=\begin{bmatrix} 0 & \frac{k_{xy}-k_{yx}}{2} \\ \frac{k_{yx}-k_{xy}}{2} & 0\end{bmatrix}, \quad (8)$$

such that $\mathbf{K}=\mathbf{K_s}+\mathbf{K_a}$.

Lemma 1. *A non-zero skew-symmetric component contributes to activity of the impedance matrix $Z(s)$.*

In fact, if one considers stiffness alone without the inclusion of higher-order dynamics, it can be shown from Condition (ii) in Definition 1 that a skew-symmetric component of stiffness will always cause the impedance to be active.

Proof. Defining $k_s \doteq \frac{k_{xy}+k_{yx}}{2}$ and $k_a \doteq \frac{k_{xy}-k_{yx}}{2}$, the velocity-to-force transfer matrix of an arbitrary stiffness matrix may be written as

$$Z(s)=\frac{1}{s}\begin{bmatrix} k_{xx} & k_s+k_a \\ k_s-k_a & k_{yy}\end{bmatrix},$$

yielding the following matrix $H(j\omega)\doteq Z(j\omega)+Z^T(-j\omega)$:

$$H(j\omega)=\frac{1}{j\omega}\begin{bmatrix} 0 & 2k_a \\ -2k_a & 0\end{bmatrix}.$$

Condition (ii) in Definition 1 requires that $H(j\omega)$ be positive semidefinite for $Z(s)$ to be passive. Since $H(j\omega)$ is Hermitian, this means its leading principal minors must be non-negative. The second principal minor of $H(j\omega)$ is $-4k_a^2/\omega^2$ which can never be non-negative (at best, it can be zero if the skew-symmetric matrix is zero), so the skew-symmetric stiffness is always active. Physically, as shown in [10], the skew-symmetric stiffness gives rise to a force field with non-zero curl, suggesting that the hand could continuously generate power by following an appropriate closed-loop trajectory.[1] □

Random measurement and identification errors *always* cause an identified stiffness to have a skew-symmetric component, even when data is collected from an array of mechanical springs that is known to be passive. Therefore, one must compare the relative magnitudes of the forces arising from the symmetric and skew-symmetric components of stiffness. If the skew-symmetric is sufficiently small, it can be attributed to random error and neglected in the passivity analysis. The relative contribution of the skew-symmetric stiffness can be assessed from the ratio of the magnitude of the skew-symmetric component of the stiffness matrix $k_a=\frac{|k_{xy}-k_{yx}|}{2}$ to the maximum and minimum eigenvalues of the symmetric stiffness ($z_{min}\doteq k_a/\lambda_{max}$ and $z_{max}\doteq k_a/\lambda_{min}$). A single skew-symmetry measure is then given by the geometric mean of these values:

$$z_{mean}=\sqrt{z_{min}z_{max}}. \quad (9)$$

Fig. 4 shows that z_{mean} was typically 25% or smaller. In his analysis of the data collected by Mussa-Ivaldi et al. in [13], Hogan found that values of z_{mean} of this size gave rise to force components that were small in comparison to those originating from the symmetric stiffness term [10]. Therefore, in the following passivity analysis, only the symmetric component of stiffness is considered .

The human operator was considered passive if the impedance $Z(s)$ in (5), comprising the identified $\mathbf{M}$, $\mathbf{B}$, and $\mathbf{K_s}$, satisfied the three conditions in Definition 1. Although Condition (ii) is defined over all frequencies, it was considered satisfied if $H(j\omega)$ was positive semidefinite from 0–10 Hz, the range of frequencies of motion observed in this study.

The results of this passivity analysis are also recorded in Table 1. All of the relaxed grasping sets were found to be passive. This agrees with Hogan's analysis, and extends his results in [10] by establishing that a relaxed grasping task is passive when a full dynamic model of impedance is employed in lieu of static stiffness alone. More importantly, while three of the 5 N rigid grasping tasks were passive, the remainder of the rigid grasping tasks were active. This clearly demonstrates that the passivity of the human arm is task-dependent. This means that, when analyzing the stability of a teleoperation system, one should not assume that the human operator behaves in a completely passive manner without analyzing the specific tasks the operator is required to perform using an approach similar to the one described in this paper.

[1] A similar analysis shows that an inertia matrix must be symmetric for passivity, while a damping matrix can be passive regardless of whether it is symmetric or not. However, when the passivity of the total system (5) comprising inertia, damping, and stiffness is considered, a small amount of skew-symmetry in the inertia can be tolerated without $H(j\omega)$ becoming negative definite over the range of frequencies relevant for human motion (0–10 Hz). Contrarily, skew-symmetry in the stiffness matrix of the total system (5) always causes $H(j\omega)$ to be negative definite in this frequency range.

Table 1: Identified human arm impedance matrices and passivity analysis results.

Task	Trial	Inertia [kg]				Damping [N·s/m]				Stiffness [N/m]				Passive/ Active
		m_{xx}	m_{xy}	m_{yx}	m_{yy}	b_{xx}	b_{xy}	b_{yx}	b_{yy}	k_{xx}	k_{xy}	k_{yx}	k_{yy}	
Relaxed Grasping	1	1.33	-1.04	-1.06	1.64	5.43	-0.60	2.10	25.51	63.59	-34.47	-57.19	324.08	P
	2	1.44	-1.09	-0.94	1.72	4.77	-2.11	-0.58	25.38	80.47	-48.07	-30.45	346.27	P
	3	1.51	-1.08	-1.13	1.92	6.47	-2.24	0.27	23.24	71.66	-39.83	-44.96	280.03	P
	4	1.71	-0.68	-1.01	1.93	6.04	-2.49	1.20	23.27	96.87	27.57	-27.74	237.24	P
	5	1.59	-1.10	-0.94	2.18	6.43	-3.61	-0.34	23.68	43.65	-35.02	7.56	252.76	P
Rigid Grasping (5 N Perturbations)	1	0.45	-1.24	-0.92	-0.54	5.15	-11.65	-2.31	20.96	187.91	-7.31	-63.25	431.08	A
	2	0.93	0.24	-1.30	2.65	10.94	-17.03	-1.56	29.97	280.26	312.80	-81.32	964.48	A
	3	0.95	-0.86	-0.50	2.15	9.42	-5.76	-7.54	34.22	308.04	-5.65	32.75	920.26	P
	4	1.23	-0.64	-1.03	1.27	7.81	-11.19	-3.97	34.74	295.23	105.73	-45.00	689.92	P
	5	0.99	-0.65	-0.69	2.04	9.77	-9.49	-3.62	23.28	301.21	193.43	1.35	888.08	P
Rigid Grasping (2 N Perturbations)	1	1.42	-0.22	-1.38	2.88	2.11	-3.73	-0.68	19.57	337.33	184.77	-86.17	879.72	A
	2	1.07	-2.22	0.09	0.57	2.94	4.51	-10.71	20.68	254.94	-202.09	74.50	583.40	A
	3	1.05	-0.10	-0.82	3.34	4.95	-13.66	-4.32	27.27	235.33	165.28	-28.67	972.27	A
	4	1.55	-1.22	-0.77	4.39	2.56	0.25	-4.36	13.79	336.72	12.84	-30.22	1038.42	A
	5	1.40	-1.54	-0.44	1.69	5.15	-6.25	-7.50	19.80	340.30	-112.70	17.66	676.15	A

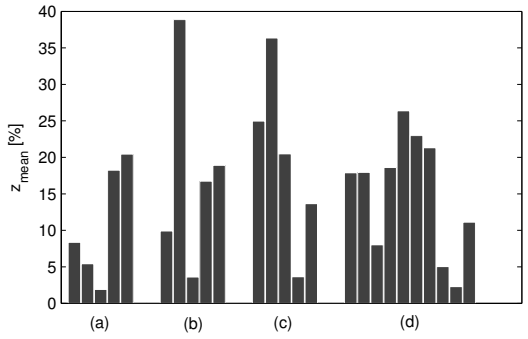

Figure 4: Percent skew-symmetry in the identified stiffness for (a) the five relaxed grasping trials, (b) the five rigid grasping trials with 5 N perturbations, and (c) the five rigid grasping trials with 2 N perturbations. For comparison, (d) shows sample skew-symmetry magnitudes from the data of Mussa-Ivaldi et al. (Table II in [13]), which were considered sufficiently small to be neglected in the passivity analysis of [10].

5 Discussion

The rigid grasping task in this paper consisted of merely resisting disturbance forces to maintain the hand at a particular position. Yet even for this simple task, the human operator was found to inject energy into the system. In many practical teleoperation applications, the human operator is required to complete much more complex movements. The assumption of human operator passivity needs to be carefully re-examined in these contexts.

It is important to emphasize that the human operator was found to behave actively for certain tasks even though a conservative analysis approach was employed that favored the conclusion of passivity. For instance, we intentionally excluded *all* skew-symmetric stiffness components, even for the two datasets with skew-symmetries in excess of 25%. However, the stiffness matrices measured for the two-dimensional arrays of springs used to validate the identification technique consistently had skew-symmetries of under 5%. Since a mechanical spring array is known to be passive in the force-velocity domain, one can reasonably argue that stiffness skew-symmetries on the order of 5% can be attributed to noise and thus neglected in passivity analysis, but skew-symmetries in excess of this threshold must be included. If the data collected in this study is reanalyzed on this basis, all but two of the data sets are found to be active, further emphasizing that the human operator cannot be assumed *a priori* to be passive without additional investigation. Similarly, the impedance was only analyzed for passivity over a limited frequency range, but including higher frequencies in the analysis results in more of the data sets being active.

Considering the human operator's time-history of energy absorption provides further insight into the task-dependent nature of passivity. When the arm is modeled as an impedance with velocity input $V = [\dot{x}\ \dot{y}]^T$ and force output $F = [f_x\ f_y]^T$ (where F is the force the robot exerts on the human), the energy absorbed by the human arm up to time t is given by $\int_0^t F \cdot v\, dt$. Fig. 5a shows a typical plot of this integral over the duration of a single perturbation in a relaxed grasping task along with the distance of the hand from the test location. We observe that, when the arm is relaxed, its impedance causes it to resist motion away from equilibrium, absorbing energy when the position perturbation displaces it from the test location. However, when the perturbation's oscillations cause the hand to move back towards the test location, there is a small decrease in the arm's energy. This is the result of the spring-like component of the arm's stiffness releasing potential energy that was stored when the arm was initially perturbed away from the test location. Nonetheless, the total energy clearly increases over the duration of the perturbation, confirming that relaxed grasping is a passive task.

For the rigid grasping tasks (Figs. 5b and 5c), the arm rapidly absorbs energy immediately after the onset of a force perturbation. As the subject cannot anticipate when the force perturbation will be applied, his reaction time (approximately 150 ms [16]) prevents him from voluntarily resisting motion during this period. Therefore, his arm absorbs energy as it is involuntarily displaced away from the test location. Once the subject realizes that his hand has been perturbed from its target position, he consciously exerts force to overcome the robot's resistance and move his hand back to the test location as quickly as possible. (Recall that the subject was instructed to prevent his hand from deviating from the test location, and not merely to slow down any motion imposed upon his hand without regard for where his hand came to rest.) This movement requires the subject to generate energy, causing the stored energy to decrease substantially. For the remainder of the perturbation, the arm's energy undergoes smaller fluctuations while the subject consciously exerts the force required to maintain his hand at the test location.

Classifying the rigid grasping task as "active" or "passive" depends on whether the energy generated in the return to the test location outweighs the energy absorbed when the hand was initially displaced away from the test location. In the 5 N force perturbation case, the robot applies a large perturbation which moves the hand

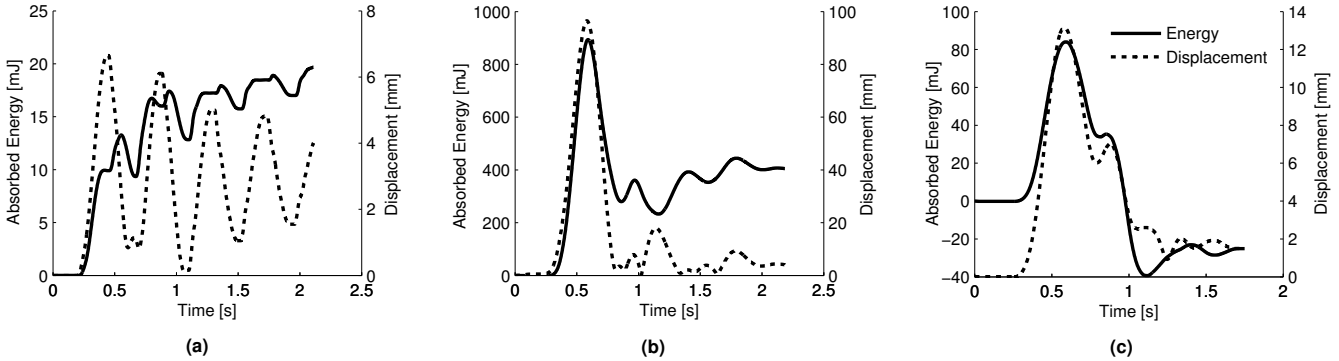

Figure 5: Typical plots of absorbed energy (solid line) and hand displacement from the test location (dashed line) for a single perturbation applied at 0.2 s in (a) relaxed grasping, (b) rigid grasping (5 N perturbation), and (c) rigid grasping (2 N perturbations). Plots show the magnitude of the two-dimensional displacement vector. The arm is assumed to have zero stored energy prior to the onset of the perturbation.

away from equilibrium at a high velocity. This causes the energy initially absorbed by the hand to be larger than the energy generated when the subject returns his hand to the target position. This task is therefore passive. For the 2 N force perturbation case, however, the robot perturbs the hand away with less force, resulting in a slower movement velocity than the 5 N case. The energy absorbed by this process is insufficient to balance the energy generated during the return movement, and the task is found to be active. This explains why the rigid grasping impedances were active for 2 N perturbations and, in a majority of cases, passive for 5 N perturbations.

Two of the 5 N rigid grasping trials were nonetheless found to be active, which emphasizes the unpredictable variations introduced to the data when the human executes a conscious position control task. The analysis approach employed in this work inherently assumed that the position control response of the CNS could be subsumed into a linear, time-invariant, second-order model (i.e., we assumed $C_h + Z_h$ can be modeled by a 2×2 inertia, damping, and stiffness transfer matrix model). While the CNS has been modeled as a linear controller in previous arm impedance studies [5], the validity of this assumption is open to question. If a more accurate parametric model of the CNS position control dynamics were developed, it could be identified in tandem with the second order model of the physical properties of the human arm.

5.1 Conclusions and Future Work

Conventional approaches to analyzing the stability of a teleoperation system using passivity-based criteria or Llewellyn's criterion necessarily assume that the human operator behaves passively. As demonstrated in this paper, this assumption does not hold for all tasks the human operator may execute and should be explicitly evaluated for the specific task in question using a method similar to the one presented here. Thus, future work in this area includes evaluating passivity with additional subjects for a broader variety of tasks to identify those for which the passivity assumption does indeed hold. In this process, more advanced models of CNS position control dynamics could be incorporated into the identification procedure to reduce inter-trial variability in the results. Finally, this work demonstrates a need for research into novel approaches to teleoperation system design and stability analysis that are capable of relaxing the requirement of human operator passivity. One possible technique is to introduce passivity observers and passivity controllers into the teleoperation system. Furthermore, in a related paper [11] we show it is possible to extend Llewellyn's criterion to the case where the human operator is active.

Acknowledgements

We gratefully acknowledge the support of the Natural Sciences and Engineering Research Council (NSERC) of Canada, Quanser Inc., and Alberta Innovates – Technology Futures.

References

[1] A. M. Acosta, R. F. Kirsch, and E. J. Perreault. A robotic manipulator for the characterization of two-dimensional dynamic stiffness using stochastic displacement perturbations. *J. Neurosci. Meth.*, 102(2):177–86, Oct. 2000.

[2] B. D. O. Anderson and S. Vongpanitlerd. *Network Analysis and Synthesis*. Prentice-Hall, 1973.

[3] R. J. Anderson and M. W. Spong. Asymptotic stability for force reflecting teleoperators with time delay. *Int. J. Robot. Res.*, 11(2):135–149, 1992.

[4] E. de Vlugt, A. C. Schouten, and F. C. T. van der Helm. Quantification of intrinsic and reflexive properties during multijoint arm posture. *J. Neurosci. Meth.*, 155(2):328–49, Sept. 2006.

[5] J. Dolan, M. Friedman, and M. Nagurka. Dynamic and loaded impedance components in the maintenance of human arm posture. *IEEE Trans. Syst. Man Cybern.*, 23(3):698–709, 1993.

[6] J. M. Dolan. *An investigation of postural and voluntary human arm impedance control*. Ph.D. dissertation, Carnegie Mellon Univ., Pittsburgh, PA, 1991.

[7] H. Gomi, Y. Koike, and M. Kawato. Human hand stiffness during discrete point-to-point multi-joint movement. In *Proc. Annu. Int. Conf. IEEE Eng.in Medicine and Biology Soc.*, pages 1628–1629, Oct. 1992.

[8] S. Haykin. *Active Network Theory*. Addison-Wesley, Reading, MA, 1970.

[9] N. Hogan. The mechanics of multi-joint posture and movement control. *Biol. Cybern.*, 52(5):315–331, Sept. 1985.

[10] N. Hogan. Controlling impedance at the man/machine interface. In *Proc. 1989 Int. Conf. Robotics and Automation*, pages 1626–1631, 1989.

[11] A. Jazayeri, M. Dyck, and M. Tavakoli. Stability analysis of teleoperation systems under stricly-passive and non-passive operator. In *IEEE World Haptics Conf. 2013*, in press.

[12] J. McIntyre, F. A. Mussa-Ivaldi, and E. Bizzi. The control of stable postures in the multijoint arm. *Exp. Brain Res.*, 110(2):248–64, July 1996.

[13] F. A. Mussa-Ivaldi, N. Hogan, and E. Bizzi. Neural, mechanical, and geometric factors subserving arm posture in humans. *J. Neurosci.*, 5(10):2732–43, Oct. 1985.

[14] J. J. Palazzolo, M. Ferraro, H. I. Krebs, D. Lynch, B. T. Volpe, and N. Hogan. Stochastic estimation of arm mechanical impedance during robotic stroke rehabilitation. *IEEE Trans. Neural Syst. Rehabil. Eng.*, 15(1):94–103, Mar. 2007.

[15] T. Tsuji, P. G. Morasso, K. Goto, and K. Ito. Human hand impedance characteristics during maintained posture. *Biol. Cybern.*, 72(6):475–85, Jan. 1995.

[16] C. Wagner and R. Howe. Mechanisms of performance enhancement with force feedback. In *Eurohaptics Conf., 2005*, pages 21–29. IEEE, 2005.